Environ Ecol Stat (2008) 15:59–70
DOI 10.1007/s10651-007-0040-1

A hierarchical Bayesian non-linear spatio-temporal model for the spread of invasive species with application to the Eurasian Collared-Dove

Mevin B. Hooten · Christopher K. Wikle

Received: 1 August 2005 / Revised: 7 July 2006 / Published online: 12 September 2007

Abstract The spread of invasive species is a long studied subject that garners much interest in the ecological research community. Historically the phenomenon has been approached using a purely deterministic mathematical framework (usually involving differential equations of some form). These methods, while scientifically meaningful, are generally highly simplified and fail to account for uncertainty in the data and process, of which our knowledge could not possibly exist without error. We propose a hierarchical Bayesian model for population spread that accommodates data sources with errors, dependence structures between population dynamics parameters, and takes into account prior scientific understanding via non-linear relationships between model parameters and space-time response variables. We model the process (i.e., the bird population in this case) as a Poisson response with spatially varying diffusion coefficients as well as a logistic population growth term using a common reaction-diffusion equation that realistically mimics the ecological process. We focus the application on the ongoing invasion of the Eurasian Collared-Dove.

Keywords Partial differential equations · Reaction-diffusion models · Invasive species

1 Introduction

Differential equation based advection-diffusion models have long been used in atmospheric science to mimic complex processes such as weather and climate. Differential and partial differential equations (PDEs) have become popular in biological and ecological fields as well. In many cases these models are considered in a strictly deterministic framework even

M. B. Hooten (✉)
Department of Mathematics and Statistics, Utah State University,
3900 Old Main Hill, Logan, UT 84322-3900, USA
e-mail: mevin.hooten@usu.edu

C. K. Wikle
Department of Statistics, University of Missouri, Columbia, MO 65211, USA

though many sources of uncertainty in the process, the model, and the measurements may exist. Specifically in the ecology realm, Clark et al. 2001 allude to a problem that arises when various sources of uncertainty are not appropriately accounted for. That is, inferences resulting from such methods will be misleading.

The spread of invasive species is one phenomenon in particular for which there is much to be (and has already been) learned about through the use of PDE models (Holmes et al. 1994; Shigesada and Kawasaki 2002). Such phenomena usually are based on complicated dynamic processes, many of which are nonlinear and are correlated with and/or controlled by other environmental features (e.g., climate patterns, biotic interactions, physiological characteristics, human population density, etc).

Many deterministic PDE models are well-equiped to represent the theoretical spread of organisms, but have no mechanism to account for the various sources of uncertainty related to the inadequacies of the model as well as the process itself and our knowledge of it. However the use of a PDE within the framework of a hierarchical Bayesian model can provide a useful link between scientifically based deterministic models and statistical models that accurately portray variability (Wikle 2003). Characterizing, and more importantly, predicting realistic levels of abundance over time depends on the models ability to recognize biologically meaningful limitations to growth, in addition to the growth rates themselves. In the early stages of an invasion, a linear growth model and density dependent growth model may behave similarly. As the carrying capacity is approached, however, a model with the flexibility to exhibit density dependence will provide more realistic results. Therefore, an invasive species model with the ability to account for non-linear growth is desirable.

Specifically, we model the spread of Eurasian Collared-Dove (ECD; *Streptopelia decaocto*) in the United States using a reaction-diffusion PDE (Fisher 1937; Skellam 1951) within a hierarchical model.

1.1 Background

The North American Breeding Bird Survey (BBS; Robbins et al. 1986) monitors many birds across the United States and Canada, and provides a major source of data for studying invasive bird species. One such species is the Eurasian Collared-Dove. The ECD is an often misidentified species in North America (due to its similarity to the Ringed Turtle-Dove) and is considered invasive and a potential threat to indigenous ecosystems (Hengeveld 1993). After moving into Europe in the 1930's, the ECD was introduced in the Bahamas and was observed in the mid-1980's in Florida (Hudson 1965; Romagosa and Labisky 2000). Not only has its range increased as it has spread through the Southeastern United States (Fig. 1), but it has experienced growth in population as well (Fig. 2).

It should be noted that these data are subject to various types of uncertainty, including observer error, spatial location error, and error related to change of spatial support (Sauer et al. 1994). Additionally, Hengeveld (1993) and Romagosa and Labisky (2000) suggest that the rate of ECD spread may vary spatially and temporally and may be correlated with other environmental covariates (e.g., human population density). Furthermore, the ECD is an important candidate for study in the United States because of the quantity of data and knowledge accumulated since its introduction combined with historical information gathered from its invasion of Europe (Hengeveld 1993).

A model that incorporates these factors and responsibly accounts for the various sources of uncertainty could be a useful tool for ecologists wanting to monitor the spread and growth in population as well as identify factors influencing the rate of spread in order to make management decisions to help protect native species.

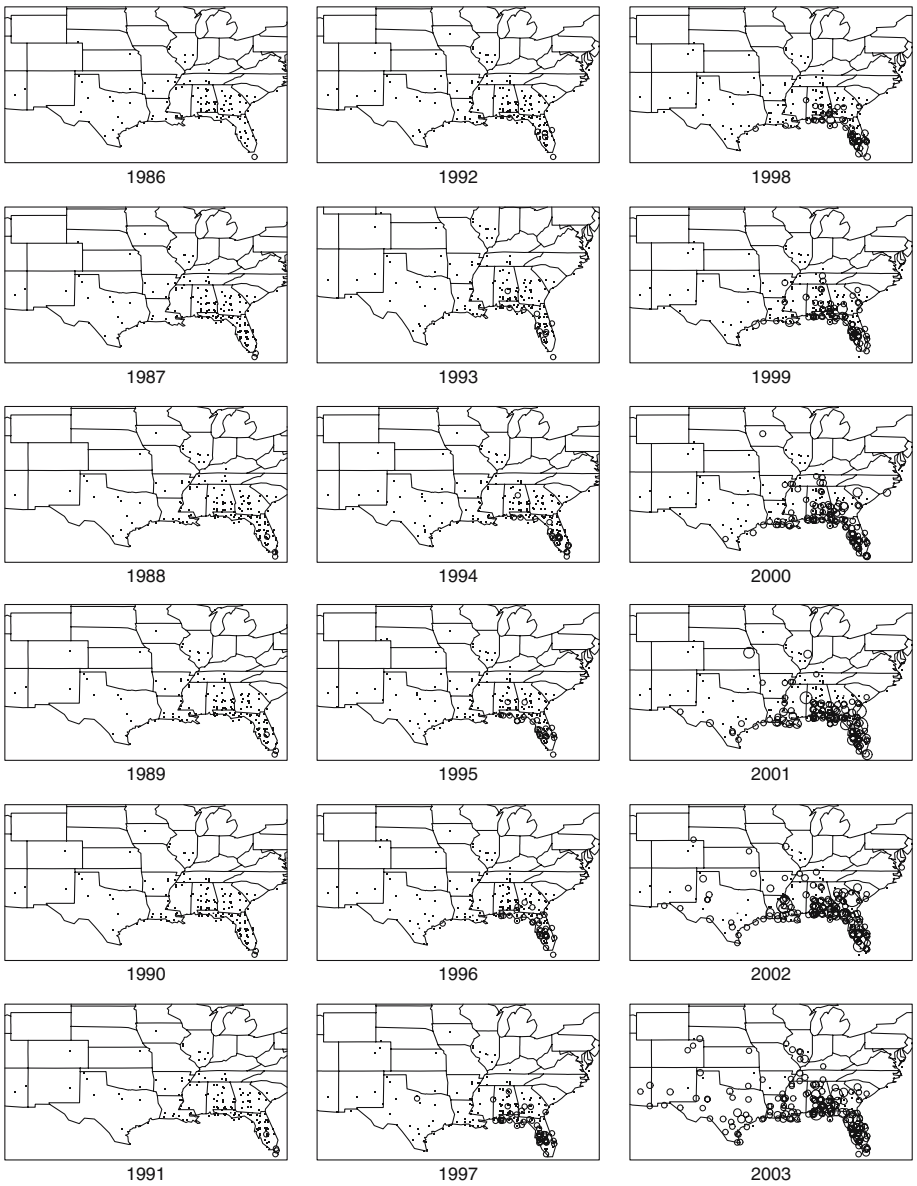

Fig. 1 Spread of ECD throughout the United States from 1986 through 2003 (points represent zero counts at sampled location, while circle size corresponds to non-zero count magnitude)

2 Methods

In order to account for the many sources of uncertainty, spatial effects, temporal effects, population growth, and spread of the invasive species we adopt a 3-stage hierarchical model that has the following factorization (Berliner 1996): [process, parameters | data] $\propto$ [data |

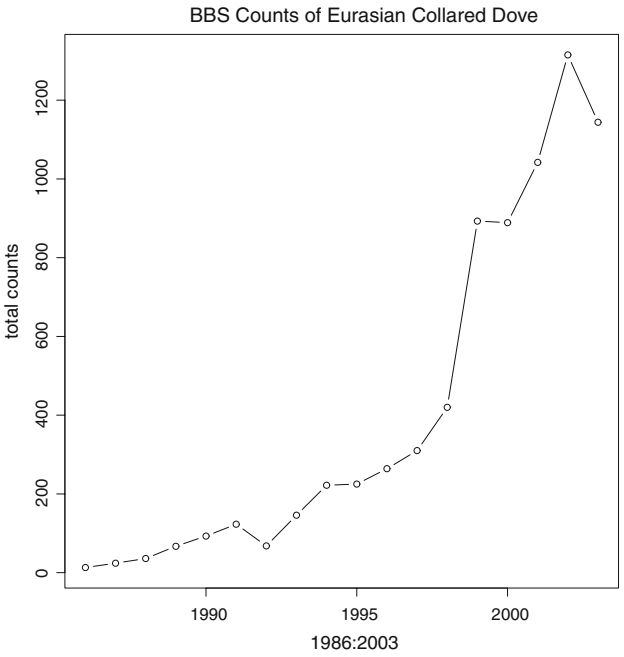

Fig. 2 Population growth of ECD in the United States from 1986 through 2003 (total counts over time)

process, parameters][process | parameters][parameters] (where the square bracket notation refers to distribution).

2.1 Data model

We consider the relative abundances of birds ($\mathbf{n}_t = [n_{1,t}, \ldots, n_{i,t}, \ldots, n_{m,t}]'$) at spatial locations $i = 1, \ldots, m$ and times $t = 1, \ldots, T$ given an intensity process as Poisson where m is the number of spatial locations and T the number of years:

$$n_{i,t}|\lambda_{i,t} \sim Pois(\lambda_{i,t}), \quad i = 1, \ldots, m \quad t = 1, \ldots, T. \tag{1}$$

In this case, the counts are originally recorded as observed along routes in the spatial domain. For our purposes, the route center is used as the point location for count data at location i. Since we are concerned about the process on the continental scale, route length (tens of kilometers) and orientation have minimal overall influence.

2.2 Process Model

The Poisson intensity process is controlled by a latent spatio-temporal process ($\mathbf{u}_t$) at gridded locations linked by an incidence matrix ($\mathbf{K}_t$). The number of gridded locations (i.e., $dim(\mathbf{u}_t) = N$) need not equal the number of observation locations; in this case $N < m$ increases computational efficiency. It may be possible to address some issues related to differences in biological processes at various scales by proposing different sets of basis functions for $\mathbf{K}_t$ but this will be left as the focus of another study. For the model proposed here, $\mathbf{K}_t$ is simply a matrix with an element in the ith row associating the ith measurement location with a grid location at time t. We use an additive independent noise term to account for observer

error and small scale spatio-temporal variability:

$$\log(\boldsymbol{\lambda}_t) = \mathbf{K}_t \mathbf{u}_t + \boldsymbol{\varepsilon}_t, \quad \boldsymbol{\varepsilon}_t \sim N(\mathbf{0}, \sigma_\varepsilon^2 \mathbf{I}), \quad t = 1, \ldots, T. \tag{2}$$

The latent process ($\mathbf{u}_t$) is motivated via a reaction-diffusion equation (Fisher 1937; Skellam 1951),

$$\frac{\partial u}{\partial t} = \frac{\partial}{\partial x}\left(\delta(x, y)\frac{\partial u}{\partial x}\right) + \frac{\partial}{\partial y}\left(\delta(x, y)\frac{\partial u}{\partial y}\right) + \gamma_0 u\left(1 - \frac{u}{\gamma_1}\right), \tag{3}$$

which can be discretized as (Haberman 1987),

$$\begin{aligned} u_t(x, y) = {} & u_{t-\Delta_t}(x, y)\left[1 - 2\delta(x, y)\left(\frac{\Delta_t}{\Delta_x^2} + \frac{\Delta_t}{\Delta_y^2}\right)\right] \\ & + u_{t-\Delta_t}(x - \Delta_x, y)\left[\frac{\Delta_t}{\Delta_x^2}\{\delta(x, y) - (\delta(x + \Delta_x, y) - \delta(x - \Delta_x, y))/4\}\right] \\ & + u_{t-\Delta_t}(x + \Delta_x, y)\left[\frac{\Delta_t}{\Delta_x^2}\{\delta(x, y) + (\delta(x + \Delta_x, y) - \delta(x - \Delta_x, y))/4\}\right] \\ & + u_{t-\Delta_t}(x, y + \Delta_y)\left[\frac{\Delta_t}{\Delta_y^2}\left\{\delta(x, y) + (\delta(x, y + \Delta_y) - \delta(x, y - \Delta_y))/4\right\}\right] \\ & + u_{t-\Delta_t}(x, y - \Delta_y)\left[\frac{\Delta_t}{\Delta_y^2}\left\{\delta(x, y) - (\delta(x, y + \Delta_y) - \delta(x, y - \Delta_y))/4\right\}\right] \\ & + u_{t-\Delta_t}(x, y)\gamma_0 - u_{t-\Delta_t}^2(x, y)\left[\frac{\gamma_0}{\gamma_1}\right], \end{aligned} \tag{4}$$

where x and y correspond to the spatial location in two dimensions. In matrix notation with additive error and letting $\Delta_t = 1$, this can be written:

$$\begin{aligned} \mathbf{u}_t = \mathbf{H}(\boldsymbol{\delta})\mathbf{u}_{t-1} + \alpha_0 \mathbf{u}_{t-1} - \alpha_1 diag(\mathbf{u}_{t-1})\mathbf{u}_{t-1} + \boldsymbol{\eta}_t, \\ \boldsymbol{\eta}_t \sim N(\mathbf{0}, \sigma_\eta^2 \mathbf{I}), \end{aligned} \tag{5}$$

where $diag(\mathbf{u}_{t-1})$ is an $N \times N$ square matrix with the elements of $\mathbf{u}_{t-1}$ on the diagonal and zeros elsewhere and γ_0 and γ_1 in (3) represent the intrinsic population growth rate and carrying capacity of the log process, respectively, and have the following relationships with the growth parameters in the vector form of the model (5):

$$\alpha_0 = \gamma_0, \quad \alpha_1 = \frac{\gamma_0}{\gamma_1}.$$

Previous models (i.e., Wikle 2003) accounted for growth in the process with a statistical trend term in the form of a random walk at a higher level in the hierarchy in addition to a Malthusian growth term in the PDE for added flexibility. Here the growth in the process is assumed to be non-linear and allows for a much more flexible model that is able to exhibit realistic biological behavior and density-dependent predictions. Additionally, if the estimate of the carrying capacity parameter (γ_1) is greater than $\mathbf{u}_t$ for all t, this would imply that the process has not stopped growing yet and estimation or prediction of abundance at times $\{t < T + 1\}$ would likely not be different than those resulting from a simpler model.

The propagator matrix ($\mathbf{H}$) in (5) depends upon the diffusion coefficients $\boldsymbol{\delta}$ which are allowed to vary in space. Construction of $\mathbf{H}$ depends on the arrangement of grid locations in the spatial domain and is thus quite project specific. For the irregularly shaped spatial domain considered here the construction of $\mathbf{H}$ is similar to that used in Wikle and Hooten (2005).

Such a non-linear model (5) is relatively difficult to implement in an MCMC (Markov Chain Monte Carlo) algorithm due to the high dimensional Metropolis-Hastings updates. Therefore, we consider the following modification (thereby also inducing a 2nd-order Markov structure).

$$\mathbf{u}_t = \mathbf{H}(\boldsymbol{\delta})\mathbf{u}_{t-1} + \alpha_0\mathbf{u}_{t-1} - \alpha_1 diag(\mathbf{u}_{t-1})\mathbf{u}_{t-2} + \boldsymbol{\eta}_t. \tag{6}$$

The $\mathbf{u}_{t-2}$ term in (6) allows for a complete derivation of the full-conditional distribution for $\mathbf{u}_t$, thereby improving computational efficiency. For a growing process such as the one considered here, the effect of using the discretization (6) of the PDE in (3) only differs from that of (5) by $\alpha_1\mathbf{u}_{t-1}|\mathbf{u}_{t-1} - \mathbf{u}_{t-2}|$. In our case, this difference is negligible and was verified by simulation. It may be possible to make exact inference on the model in (5) using (6) as a proposal in a Metropolis-Hastings step. The resulting model is the subject of ongoing research.

2.3 Parameter model

Let $\mathbf{X}$ be an $N \times 2$ covariate matrix made up of an intercept and human population density on the gridded spatial domain and let $\boldsymbol{\beta}$ be a 2-dimensional vector of regression coefficients with $\mathbf{R}$ a spatial correlation matrix depending on parameter θ. Then, $\boldsymbol{\delta}$ can be defined by a linear model,

$$\boldsymbol{\delta} = \mathbf{X}\boldsymbol{\beta} + \boldsymbol{\xi}, \quad \boldsymbol{\xi} \sim N(\mathbf{0}, \sigma_\delta^2\mathbf{R}(\theta)). \tag{7}$$

Let the spatial correlation matrix ($\mathbf{R}$) be defined by the distance ($||d||$; the Euclidian distance between points) and the spatial range parameter (θ) in the standard stationary and isotropic exponential covariogram model:

$$R(\theta, d) = exp(-\theta||d||). \tag{8}$$

This allows $\boldsymbol{\delta}$ to utilize not only the human population covariate but the (random) effects of another spatial covariate possibly based on an unknown environmental factor. Also, we let the ECD population growth parameters have a lognormal distribution:

$$\log(\boldsymbol{\alpha}) \equiv \log\left(\begin{bmatrix}\alpha_0\\ \alpha_1\end{bmatrix}\right) \sim N(\tilde{\boldsymbol{\alpha}}, \boldsymbol{\Sigma}_\alpha). \tag{9}$$

The remaining parameters have the following priors:

$$\boldsymbol{\beta} \sim N(\boldsymbol{\beta}_0, \boldsymbol{\Sigma}_\beta), \tag{10}$$

$$\sigma_\varepsilon^2 \sim IG(q_\varepsilon, r_\varepsilon), \tag{11}$$

$$\sigma_\eta^2 \sim IG(q_\eta, r_\eta), \text{ and} \tag{12}$$

$$\sigma_\delta^2 \sim IG(q_\delta, r_\delta). \tag{13}$$

We specify a prior distribution for the $\mathbf{u}_t$-process at time zero, $\mathbf{u}_0 \sim N(\tilde{\mathbf{u}}_0, \boldsymbol{\Sigma}_0)$ and let $\mathbf{u}_{-1} = -10 \times \mathbf{1}$ be fixed (where $\mathbf{1}$ is a vector of ones). It is reasonable to fix $\mathbf{u}_{-1}$ at a small value because it represents the process at a time before the invasion began; about which there is little uncertainty. Finally, we adopt a reference prior for the spatial parameter θ as derived by Berger et al. (2002). Such a reference prior is non-informative and more importantly allows the posterior to be proper. Prior distributions (9–13) were chosen to ensure model conjugacy for purposes of computational and analytical efficiency, while hyperparameters were either chosen to ensure vague priors or, if sufficient information was available, based on previous studies (e.g., rates of ECD spread in Europe). Table 1 shows the numerical values used for the hyperparameters.

Table 1 Hyperparameters used in MCMC

Hyperparameter	Value
q_ε	2.3
r_ε	0.4
q_η	2.0
r_η	2.0
q_δ	2
r_δ	1,000
$\tilde{\alpha}_0, \tilde{\alpha}_1$	0.001
$(\boldsymbol{\Sigma}_\alpha)_{11}, (\boldsymbol{\Sigma}_\alpha)_{22}$	10
$(\boldsymbol{\Sigma}_\alpha)_{12}, (\boldsymbol{\Sigma}_\alpha)_{21}$	2
$\tilde{\mathbf{u}}_0$	$\mathbf{0}$
$\boldsymbol{\beta}_0$	$\mathbf{0}$
$\boldsymbol{\Sigma}_0, \boldsymbol{\Sigma}_\beta$	$10 \times \mathbf{I}$

The Bayesian formulation of the hierarchical model is summarized by the following posterior distribution and does not have an analytical representation.

$$\begin{aligned}
&[\boldsymbol{\lambda}_1, \ldots, \boldsymbol{\lambda}_T, \mathbf{u}_0, \ldots, \mathbf{u}_T, \boldsymbol{\delta}, \boldsymbol{\alpha}, \boldsymbol{\beta}, \sigma_\epsilon^2, \sigma_\eta^2, \sigma_\delta^2, \theta | \mathbf{n}_1, \ldots, \mathbf{n}_T] \\
&\quad \propto \left\{ \prod_{t=1}^{T} [\mathbf{n}_t | \boldsymbol{\lambda}_t][\boldsymbol{\lambda}_t | \mathbf{u}_t, \sigma_\epsilon^2] \right\} \left\{ \prod_{t=1}^{T} [\mathbf{u}_t | \boldsymbol{\delta}, \mathbf{u}_{t-1}, \mathbf{u}_{t-2}, \boldsymbol{\alpha}, \sigma_\eta^2][\mathbf{u}_0] \right\} \\
&\qquad \times [\boldsymbol{\delta} | \boldsymbol{\beta}, \sigma_\delta^2, \theta][\boldsymbol{\alpha}][\boldsymbol{\beta}][\sigma_\epsilon^2][\sigma_\eta^2][\sigma_\delta^2][\theta]. \qquad (14)
\end{aligned}$$

Therefore, a Gibbs sampler was used to sample from the posterior using the relevant full-conditional distributions. Additionally, non-conjugate parameters $\{\boldsymbol{\lambda}_t : t = 1, \ldots, T\}$ and θ, are sampled via Metropolis-Hastings updates within the Gibbs sampler.

3 Results

This section contains results of the MCMC output and analysis; a discussion of the results follows in the next section. Additionally, for the purpose of illustration only, all remaining maps based on model output are shown as images, where the grid locations correspond to pixel centers. The Gibbs sampler was run for 200,000 iterations with a burn-in of 20,000 iterations to ensure convergence of the parameter chains. We can visualize the marginal posterior distribution of model parameters by viewing the histograms constructed from the MCMC samples (Fig. 3).

Figure 4 shows the posterior mean and standard deviation of the spatial diffusion coefficient ($\boldsymbol{\delta}$) in the form of a map on the spatial domain. The human population covariate (in $\mathbf{X}$) is also shown in Fig. 4 for comparison.

One way to view the change over time in the Poisson intensity parameter is to plot the posterior mean and 95% credible interval at a location of interest. Consider ECD growth at a South Florida location (Fig. 5). Additionally, by utilizing the MCMC samples from the spatial parameters (σ_δ^2, θ), we can construct a posterior covariogram (assuming the covariogram model in (8)) with 95% credible interval to give us some idea of the spatial structure in $\boldsymbol{\delta}$ beyond that available in the covariate matrix ($\mathbf{X}$) (Fig. 5). We can also view these intensity parameters ($\boldsymbol{\lambda}$) on the spatial domain as a series of maps over time (Fig. 6). Additionally, consider the posterior prediction for $\boldsymbol{\lambda}$ (Fig. 7).

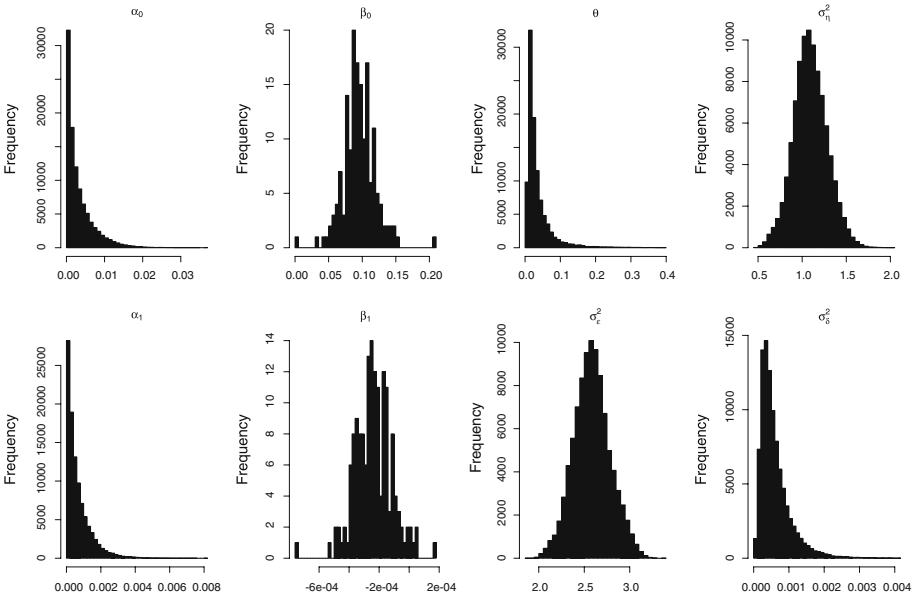

Fig. 3 Posterior distributions of bivariate parameters ($\boldsymbol{\alpha}$, $\boldsymbol{\beta}$) and univariate (θ, σ^2_ε, σ^2_η, σ^2_δ)

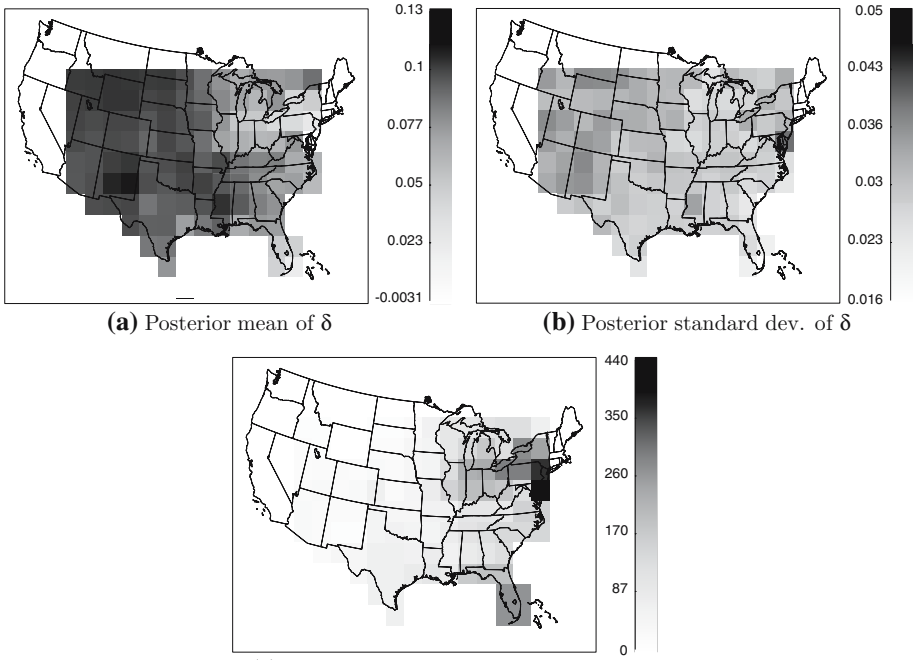

(a) Posterior mean of δ

(b) Posterior standard dev. of δ

(c) Human population covariate map (i.e., 2nd column of **X**).

Fig. 4 Posterior summary of $\boldsymbol{\delta}$ and covariate. (**a**) Posterior mean of $\boldsymbol{\delta}$. (**b**) Posterior standard dev. of $\boldsymbol{\delta}$. (**c**) Human population covariate map (i.e., 2nd column of **X**)

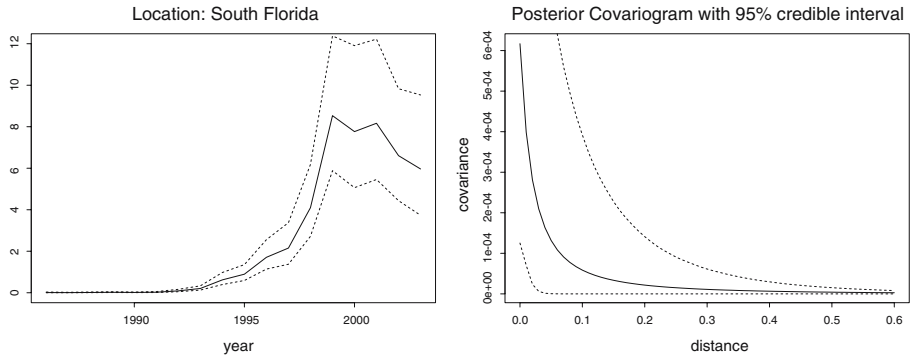

(a) Posterior mean (and 95% credible interval) of the Poisson intensity process at a South Florida location through time (represents ECD population growth).

(b) Posterior covariogram with 95% credible intervals (i.e., covariance structure of $\boldsymbol{\xi}$). Maximum distance in the covariogram equals maximum map distance.

Fig. 5 Posterior summary of $\boldsymbol{\lambda}$ and $\boldsymbol{\xi}$. (**a**) Posterior mean (and 95% credible interval) of the Poisson intensity process at a South Florida location through time (represents ECD population growth). (**b**) Posterior covariogram with 95% credible intervals (i.e., covariance structure of $\boldsymbol{\xi}$). Maximum distance in the covariogram equals maximum map distance

4 Discussion

It appears that human population density is negatively associated with the rate of diffusion, however the association is only borderline significant (Figs. 3, 4), although the intercept coefficient in $\boldsymbol{\beta}$ is clearly significant, suggesting that at least a mean term is important in the model. The negative association is somewhat contrary to popular scientific opinion, although it could be that ECD relative abundance, rather than rate of diffusion, is more strongly correlated with human proximity. Note also that a few samples of $\boldsymbol{\delta}$ were negative (Fig. 4). Technically, $\boldsymbol{\delta}$ should not take negative values, however in this case the model is flexible enough to allow $\boldsymbol{\delta}$ to be negative to make up for other possible deficiencies or misspecifications. Specifically, the human population covariate (Fig. 4) contains an outlier and its linear relationship with $\boldsymbol{\delta}$ forces it to be negative. Due to its magnitude, the effect of such an artifact is minimal.

On the other hand, the spatial parameters $(\sigma_\delta^2, \theta)$ influencing the variability in rate of diffusion are significant (Fig. 3) suggesting that diffusion is affected by some underlying process (e.g., an unknown latent spatial covariate such as land type, temperature, or precipitation) and are useful in modeling ECD relative abundance in time and space. The covariogram in Fig. 5 illustrates that significant spatial structure exists within approximately one third of the maximum map distance; in fact, most (i.e., 95%) of the spatial structure lies within 1/6th of the maximum map distance (i.e., 1/6th the width of the United States). This implies that the variability associated with the rate of diffusion that is not attributed to human population is likely due to some unknown spatial covariate with a range of spatial dependence equal to 0.1 in map distance and (or) due to the biological characteristics of ECD dispersal.

The posterior mean (at most locations) of the Poisson intensity process (e.g., Fig. 5) generally shows an increasing trend over time as we would expect and could indeed be the driving force behind the measurements $(\mathbf{n}_t)$. Some locations have an initial decrease in intensity that could be due to an Allee effect (Shigesada and Kawasaki 2002) not present in the original data. Recall that this intensity process is controlled by an underlying latent process $(\mathbf{u}_t)$

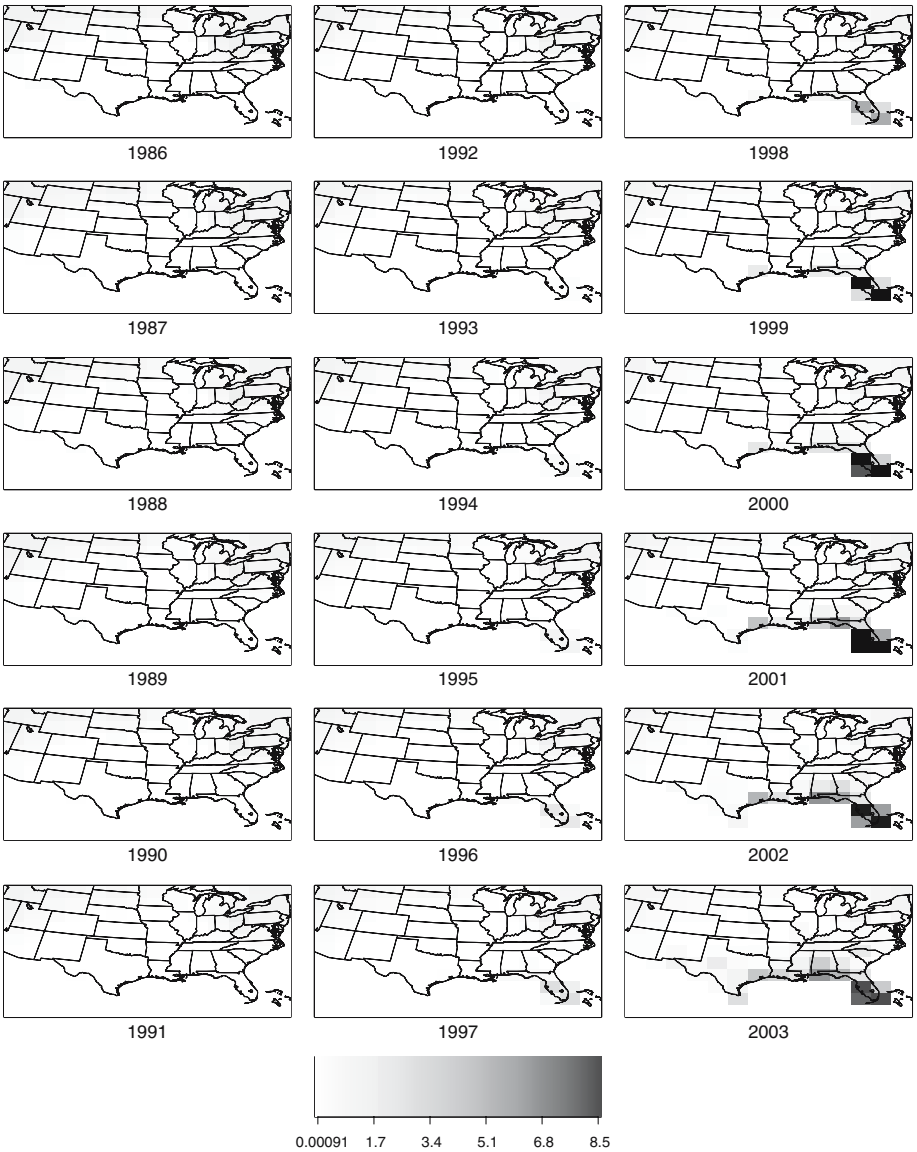

Fig. 6 The posterior mean of the Poisson intensity process in time and space

and thus appears similar (Fig. 6) over space and time as σ_η^2 is quite small and the growth parameters in the PDE are only weakly influential (Fig. 3). Moreover, as with similar models (e.g., Wikle 2003), the process is mostly data-driven and the growth component (although possibly misspecified) allows ample flexibility for modeling the relative abundance as well as non-linear population growth and diffusion.

The prediction for the Poisson intensity process (i.e., mean relative ECD abundance) may be useful for managers wishing to control future range expansion of this species and compare with future monitoring efforts. Notice however that there exists a substantial amount

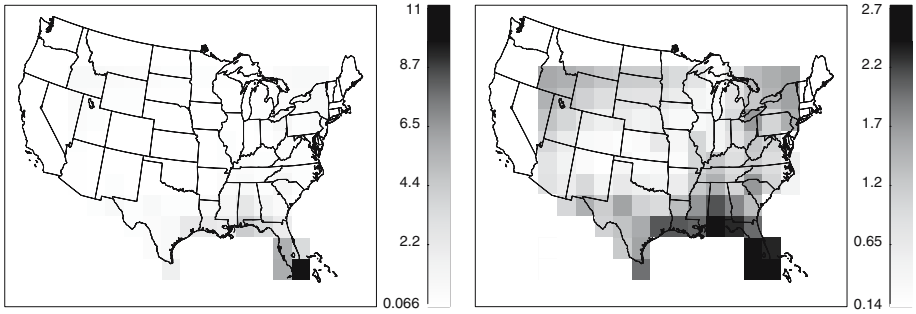

(a) Posterior mean for Poisson intensity prediction.

(b) Posterior standard deviation for Poisson intensity prediction.

Fig. 7 Posterior prediction of λ for 2004. (**a**) Posterior mean for Poisson intensity prediction. (**b**) Posterior standard deviation for Poisson intensity prediction

of uncertainty in the prediction (Fig. 7), accurate knowledge of which may not be available through other conventional prediction methods.

5 Conclusions

The ecology of invasive species is complicated, with non-linear non-seperable spatio-temporal variation influencing the amount of growth and rate of spread of which our knowledge is affected by measurement error and various other sources of uncertainty. We have implemented an ecologically meaningful PDE within a hierarchical Bayesian framework as a latent dynamical system to help manage such uncertainty and account for complicated dependence structures in parameters.

Specifically, inference based on this model suggests that not only does correlation exist between ECD abundance in space and time but the growth and spread of this species across North America can be described and predicted (even at locations without data) while accurately and responsibly accounting for uncertainty. It is important to note that the reaction-diffusion model for the latent process here is one that represents scientific opinion. However, it is by no means the only way to incorporate scientific knowledge into the model. In fact, matrix models (Caswell 2001) may prove to be a promising tool in future invasive species research efforts. Such settings allow for the inclusion of well-known non-linear growth and dispersal equations acting upon a more intuitive latent process. Implementation of these models, however, presents a variety of challenges.

References

Berger J, De Oliveira V, Sanso B (2002) Objective Bayesian analysis of spatially correlated data. J Am Stat Assoc 96:1361–1374

Berliner L (1996) In: Hanson K, Silver R (eds) Maximum entropy and bayesian methods. Hierarchical Bayesian time series models. Kluwer Academic Publishers, pp 15–22

Caswell H (2001) Matrix population models. Sinauer Associates, Inc., Sunderland, MA

Clark J, Carpenter S, Barber M, Collins S, Dobson A, Foley J, Lodge D, Pascual M, Pielke R Jr, Pizer W, Pringle C, Reid W, Rose K, Sala O, Schlesinger W, Wall D, Wear D (2001) Ecological forecasts: an emerging imperative. Science 293:657–660

Fisher R (1937) The wave of advance of advantageous genes. Ann Eugen 7:355–369
Haberman R (1987) Elementary applied partial differential equations. Prentice Hall, Inc., Englewood Cliffs, NJ, USA
Hengeveld R (1993) What to do about the North American invasion by the Collared Dove? J Field Ornithol 64:477–489
Holmes E, Lewis M, Banks J, Veit R (1994) Partial differential equations in ecology: spatial interactions and population dynamics. Ecology 75:17–29
Hudson R (1965) The spread of the Collared Dove in Britain and Ireland. Br Birds 58:105–139
Robbins C, Bystrak D, Geissler P (1986) The breeding bird survey: its first fifteen years, 1965-1979. Fish and Wildlife Service Resource Publication 157, USDOI, Washington, DC, USA
Romagosa C, Labisky R (2000) Establishment and dispersal of the Eurasian Collared-Dove in Florida. J Field Ornithol 71:159–166
Sauer J, Peterjohn B, Link W (1994) Observer differences in the North American breeding bird survey. Auk 111:50–62
Shigesada N, Kawasaki K (2002) In: Bullock J, Kenward R, Hails R (eds) Dispersal ecology, invasion and the long range expansion of species: effects of long-distance dispersal. Blackwell Publishing, Malden, Massachusetts
Skellam J (1951) Random dispersal in theoretical populations. Biometrika 38:196–218
Wikle C (2003) Hierarchical Bayesian methods for predicting the spread of ecological processes. Ecology 84:1382–1394
Wikle C, Hooten M (2005) In: Clark JS, Gelfand (eds) Applications of computational statistics in the environmental sciences: hierarchical Bayes and MCMC methods. Hierarchical Bayesian spatio-temporal models for population spread. Oxford University Press

Author Biographies

Mevin B. Hooten earned BS and MS degrees from Kansas State University in Natural Resources (1999) and the University of Missouri—Columbia in Forestry (2001), respectively. He then obtained a PhD in Statistics (2006) from the University of Missouri—Columbia, with dissertation research focusing on hierarchical spatio-temporal statistical models for ecological processes. He is currently an Assistant Professor of Statistics in the Department of Mathematics and Statistics, a Faculty Associate of the Ecology Center, and an Adjunct Faculty Member in the Department of Wildland Resources at Utah State University. His research interests are in the development and application of spatial, temporal, and spatio-temporal models for natural systems and the interface between applied mathematics and statistics.

Christopher K. Wikle obtained BS and MS degrees in atmospheric science from the University of Kansas in 1986 and 1989, respectively. From 1988 to 1991 he worked as an air pollution consultant, primarily studying potential environmental impacts of proposed power generation facilities. He then obtained an MS in statistics at Iowa State University in 1994 and a co-major PhD in both atmospheric science and statistics at Iowa State University in 1996. From 1996 to 1998 he was a visiting scientist in the Geophysical Statistics Project at the National Center for Atmospheric Research in Boulder, Colorado. He is currently Associate Professor of Statistics and Adjunct Professor of Atmospheric Science at the University of Missouri, Columbia. He was elected Fellow of the American Statistical Association in 2004. His research interests are in the application of statistics to geophysical and environmental processes. Specific interests include spatio-temporal models, hierarchical Bayesian methods, the introduction of physical information into stochastic models, statistical design of environmental monitoring networks, climate dynamics, atmospheric waves, nowcasting, ecology, and models for invasive species.